Disentangling Mnemonic Metacognition from Confidence by Communication between the Precuneus and Hippocampus

Kai Pan*[1,2], Xinxia Guo*[1,2], Zhe Zheng[1,2], Zhoule Zhu[1,2], Hemmings Wu[1,2], Junming Zhu[1,2], Diogo Santos-Pata[5], Jianmin Zhang[1,2,3,4], Sze Chai Kwok[5,6,7,8,9], Hongjie Jiang[1,2]

[1] The second affiliated hospital of Zhejiang University School of Medicine, Hangzhou, Zhejiang, China
[2] Key Laboratory of Precise Treatment and Clinical Translational Research of Neurological Diseases, Hangzhou, Zhejiang, China
[3] Brain Research Institute, Zhejiang University, Hangzhou, Zhejiang, China
[4] Collaborative Innovation Center for Brain Science, Zhejiang University, Hangzhou, Zhejiang, China
[5] Phylo-Cognition Laboratory, Division of Natural and Applied Sciences, Data Science Research Center, Duke Kunshan University, Duke Institute for Brain Sciences, Kunshan, Jiangsu, China
[6] Shanghai Key Laboratory of Brain Functional Genomics, Key Laboratory of Brain Functional Genomics (Ministry of Education), Shanghai Key Laboratory of Magnetic Resonance, Affiliated Mental Health Center (ECNU), School of Psychology and Cognitive Science, East China Normal University, Shanghai, China
[7] State Key Laboratory of Cognitive Neuroscience and Learning, Beijing Normal University, Beijing, China
[8] Shanghai Key Laboratory of Magnetic Resonance, East China Normal University, Shanghai, China
[9] Shanghai Changning Mental Health Center, Shanghai, China

Correspondence

(1) Hongjie Jiang, Department of Neurosurgery, Second Affiliated Hospital, School of Medicine, Zhejiang University, 88 Jiefang Road, Hangzhou, Zhejiang 310009, China. Email: insjhj@zju.edu.cn

(2) Sze Chai Kwok, Duke Kunshan University No. 8 Duke Avenue, Kunshan, Jiangsu, 215316 China. Email: sze-chai.kwok@st-hughs.oxon.org

(3) Jianmin Zhang, Department of Neurosurgery, Second Affiliated Hospital, School of Medicine, Zhejiang University, 88 Jiefang Road, Hangzhou, Zhejiang 310009, China. Email: zjm135@zju.edu.cn

Kai Pan and Xinxia Guo authors contributed equally to this work.

ABSTRACT

Metacognition, the ability to introspectively monitor confidence prior to decision-making, remains an area with unclear neural mechanisms, particularly concerning the intercommunication among various brain regions. Recently, the precuneus has emerged as a key player in mnemonic metacognitive tasks, while the hippocampus's involvement in memory function is well-established. Our study sought to examine the roles of the precuneus and hippocampus in mnemonic metacognition, employing intracranial electrode recordings from patients with intractable epilepsy to analyze the regulatory and correlational dynamics between these regions. We identified distinct communication patterns between the precuneus and hippocampus during metacognition and confidence generation. Furthermore, we conducted a quantitative assessment of the temporal dynamics involved in metacognition and the generation of confidence. Our observations reveal that introspective judgments typically occur subsequent to the generation of confidence. Our study sheds light on the neural underpinnings of metacognition and the genesis of confidence, focusing on the interplay between the hippocampus and the precuneus. This investigation lays the groundwork for deepening our comprehension of the nuances distinguishing confidence from metacognition.

INTRODUCTION

Metacognition, defined as the ability to introspectively monitor and regulate cognitive processes, fundamentally involves reevaluating cognition and objectively assessing confidence in decision-making (Flavell, 1979). Confidence is predominantly evidenced through the certainty displayed in the performance of tasks, whereas metacognition pertains to the individual's beliefs and knowledge within real-world contexts (Fleming, 2024; Miyoshi et al., 2024). While efforts have been made to develop models for computing propositional confidence, aimed at differentiating between confidence and metacognition (Pouget et al., 2016; Fleming & Daw, 2017), definitive electrophysiological evidence supporting the distinction between these two processes remain unrevealed.

A multitude of studies have delineated the neural underpinnings of various domains of metacognition, particularly in relation to perception and memory. These investigations have delineated a more pronounced association of the prefrontal cortex with perception-related metacognition, whereas the precuneus appears to be more intricately linked with memory-related metacognition (Fleming et al., 2010; McCurdy et al., 2013; Baird et al., 2013). Despite advances in identifying the critical roles of the prefrontal (Hebart et al., 2016; Shekhar and Rahnev, 2018; Cai et al., 2022) and parietal cortices (Morales et al., 2018; Pereira et al., 2021) in metacognitive processes, the communication between multiple regions underlying the computation for confidence and metacognition remain elusive.

The precuneus has been implicated not only in metacognitive processes related to memory but also plays a significant role in memory functions. Studies have shown its involvement in maintaining object-location within working memory (Bicanski & Burgess, 2018), facilitating the retrieval of autobiographical memories (Hebscher et al., 2020), and reconstructing contextual information to aid temporal order memory tasks (Foudil et al., 2020). Given the precuneus's integral role in memory-related cognitive

processes and its anatomical connection with the hippocampus (Tanglay et al., 2022), we hypothesized the existence of a neural circuit linking the precuneus and the hippocampus. Empirical evidence supports this hypothesis, documenting hippocampal-precuneus connections that can predict memory retrieval confidence levels (Ren et al., 2018) as well as the importance of hippocampal to posterior parietal cortex information flow in episodic memory tasks (Das and Menon, 2023). The pathway between the hippocampus and the precuneus has also been implicated in reasoning decision processes (Pudhiyidath et al., 2023) and in self- and goal-oriented processing (Zheng et al., 2021). The involvement of the hippocampal-parietal circuits underpinning these related processes in higher cognition implied that the communication between the hippocampus and precuneus would also be important for memory-related metacognition. To date, one study has demonstrated that increased resting-state functional connectivity (rs-fcMRI) between the precuneus and the hippocampus is significantly associated with metamemory ability (Ye et al., 2019).

Previous research, which has predominantly utilized magnetic resonance imaging, animal neurophysiology, or cognitive alterations under pathological states, has yet to definitively ascertain alterations in neural electrical activity within the human brain during mnemonic metacognitive processes. Our study seeks to address this lacuna by analyzing intracranial electroencephalogram signals from patients with intractable epilepsy, aiming to uncover the correlation and potential neural pathways linking the precuneus and hippocampus within mnemonic metacognition. To more precisely define confidence and metacognition, our research adopts methodologies grounded in the signal detection theory (SDT) framework (Maniscalco and Lau, 2012) and the hierarchical Bayesian estimation technique (Fleming, 2017). By synthesizing behavioral and electrophysiological signal analyses, our study endeavors to delineate the unique neural mechanisms that underpin confidence and metacognition, thereby contributing to a deeper understanding of these intricate cognitive processes.

RESULT

A total of eight patients underwent stereoelectroencephalography (sEEG) surgery for intractable epilepsy, and their brain electrical signals during metacognitive behavioral tasks were recorded and collected postoperatively. There are basic information and clinical characteristics of the eight subjects (Supplementary Table S1). Metacognitive cognitive behavioral testing was conducted for all subjects in the postoperative ward. Initially, the patients were instructed to watch a video and subsequently asked to determine the temporal order of occurrence between two displayed pictures in the video. After each memory judgment, they were required to make a confidence judgment (Fig.1a, see Methods section for further details). The localization of the electrodes (Fig. 1b) in specific brain regions was determined using preoperative MRI (Fig. 1c).

Behavioral results

We calculated the mean levels of confidence (3.58±0.19 mean±SEM) and accuracy (0.79±0.094 mean±SEM) for eight participants throughout the behavioral experiment (Fig. 1d). After classifying according to the level of confidence, we found that trials with high confidence had significantly higher accuracy compared to trials with low confidence (Fig. 1e, p=0.078, paired signed-rank test). Reaction times were significantly shorter in the high confidence×correct trials than in the low confidence×incorrect trials (Fig. 1f, p=0.0117, Friedman test, multiple comparisons) during the retrieval stage, but not significant in the confidence stage (Fig. 1g, p=0.3476, Friedman test). There was a significant positive correlation between accuracy and confidence level across sessions (Fig. 1h, r=0.3600, p=0.0177, pearson correlation) with a gradual improvement across multiple sessions (Fig. 1i).

Precuneus and hippocampus are involved in confidence generation through phase-amplitude coupling

The LFP analysis focused on twelve electrodes located in the precuneus and eight electrodes in the hippocampus. First, we utilized the phase amplitude coupling (PAC) method to evaluate the communication between the precuneus and hippocampus in metacognition. The PAC across these regions were shown in Fig.2a during three stages: retrieval, fixation, and confidence rating. A strong interaction was observed between the low frequency in the precuneus and the amplitude of high frequency in the hippocampus during the confidence rating stage compared with other stages. Furthermore, the phase distribution during this stage differed from the other two stages taking one trial as an example (Fig. 2b). Subsequently, we conducted a comparison of the PAC between trials with high and low confidence levels within the high frequency band (30-200 Hz) and low frequency band (4-30Hz) for each participant and discovered that the modulation index was significantly higher during the confidence rating stage than in the preceding stages (Fig.2c; $p=0.0066$ for retrieval, $p<0.0001$ for fixation, Friedman test). The trends in modulation index are consistently distinct between the three stages of the study for the 12 precuneus sites recorded from the 8 subjects (Fig. 2d), thus supporting a consistent pattern.

To more accurately determine whether this coupling is associated with the confidence generation and metacognition, we organized trials based on confidence levels (Fig. 3a) and that trials with high confidence exhibited a significantly stronger PAC in comparison to trials with low confidence (Fig. 3b, $p=0.0269$, paired signed-rank test). However, when we combined the classification based on correctness of responses, we found no significant differences between groups (Supplementary Fig. S1). Then we analyzed the correlation between phase amplitude coupling and metacognitive efficiency and no significant correlation was found between M-ratio and modulation index (Supplementary Fig. S1). The findings revealed a significantly higher coupling phenomenon in trials with high confidence. However, this high level of phase amplitude coupling effect does not seem to relate to the metacognitive efficiency of the participants. Therefore, we consider this higher coupling phenomenon to be part of the

neural mechanism in the generation of confidence.

High frequency band in hippocampus is more related to metacognitive efficiency compared with the precuneus

Observations indicate a notable disparity in the coupling strength during trials characterized by high versus low levels of confidence. This prompted an analysis to ascertain whether this variation in coupling strength correlates with the energy across different frequency bands in the precuneus and the hippocampus. In the precuneus, an increased activation in the low frequency band was observed in participants reporting high confidence, as opposed to those with low confidence (Fig.4a). Subsequently, we analyzed the power spectral density (PSD) of the precuneus during the entire confidence reporting stage. Upon classifying trials based on high or low confidence levels, it was evident that high confidence trials exhibited markedly higher energy in the low frequency band, particularly within the delta and theta frequency bands, in contrast to low confidence trials (Fig.4b, delta: $p=0.0161$; theta: $p=0.0005$, paired sign-rank test). However, no significant differences were observed in other frequency bands during the confidence rating stage (Supplementary Fig. S2). To further investigate whether the precuneus effect metacognitive efficiency, we calculated the M-ratio (meta-d'/d') for each subject. We found no significant correlation observed between the M-ratio and theta activity in the precuneus (Fig.4c).

In the hippocampus, when assessing high confidence relative to low confidence, we noted a decline in high frequency activity in the hippocampus (Fig. 4d). When classifying trials based on high and low confidence levels, we observed significant differences in high gamma frequency, with low confidence trials exhibiting higher energy than high confidence trials (Fig.4e, $p=0.0078$, paired sign-rank test). No other frequency bands exhibited significance in differentiating confidence levels during the confidence rating stage (Supplementary Fig. S3). Intriguingly, we also a significant negative correlation between the M-ratio and high gamma activity (Fig.4f, $r=-0.7341$,

p=0.0381, pearson correlation). In this respect, we showed a functional dissociation between the precuneus and the hippocampus.

Elevated correlation between the precuneus and hippocampus gamma frequency in metacognitive processes

Having established the relationship between the high gamma band activity of the hippocampus and metacognitive efficiency, we looked into how hippocampal gamma band might work with that of the precuneal sites. We applied a correlation analysis method to determine whether a specific correlation exists between the precuneus and the hippocampus within the high gamma frequency band. Utilizing a window width of 0.04s and steps of 0.02s, we computed the Pearson correlation coefficient for the hippocampus and precuneus signals. Significantly correlated amplitude segments with a length greater than 0.08s were considered (Fig.5a). We conducted the correlation analysis for each participant and tested the result against correlation values obtained from shuffled trials as a baseline. The results involving all participants indicated a significant elevation in the area under the curve (AUC) in the original data compared to the shuffled data (Fig.5b, $p<0.0001$, paired t-test). We noted a significantly higher count of correlations in comparison to the baseline (see example subject, Fig.5c). Both positive and negative correlations exhibited significantly higher values than the baseline. Next, we found that trials with higher confidence levels exhibited a significantly higher proportion of positive correlations compared to trials with lower confidence levels (Fig.5e, $p<0.0001$, Chi-square test), but the count between high and low confidence had no difference (Fig.5d). Furthermore, to assess correlation in metacognition, we classified the data based on the accuracy of responses. Our observations revealed a higher proportion of positive correlations associated with confidence levels, regardless of whether the responses were correct (Fig.5f, $p<0.0001$, Chi-square test). Next, we classified the data by the accuracy of the responses only. We found an increase in the count of correlations in the incorrect trials compared to the correct trials (Fig.5g, $p=0.022$, paired t-test). Unlike the results in confidence level,

there was no difference in correlation proportion between correct and in correct (Fig.5h). When classifying the trials based on correctness and confidence, there were no significant differences observed in count between groups (Supplementary Fig. S4). Importantly, to further validate the relationship between the high level of correlation and metacognitive efficiency, we performed correlation analyses between the count and proportion of correlation and the M-ratio for each participant. Our findings revealed a significant correlation between both variables and M-ratio (Fig. 5i, 5j, proportion: $r=0.7426$, $p=0.0345$; count: $r=0.7098$, $p=0.0486$). The above results reveal that the hippocampus and precuneus participate in the metacognitive process interactively, via a crosstalk in the high gamma band.

The correlation of metacognition between precuneus and hippocampus exhibited a delay compared with confidence generation

Our sEEG data allow us to investigate the time course of metacognition computation with a very high temporal resolution. We employed the correlation analysis method to determine the change in the correlation coefficient of the first second of confidence rating stage using a window width of 0.04s. Initially, the trials were categorized based on confidence levels and compared across each time point. A significant difference was observed around 0.4s (Fig. 6a, $p=0.0399$, t-test). The vertical line indicating the time point with the highest t-value within each participant and the color represents different p-value levels (red: $p<0.05$, orange: $p<0.1$, black: $p>0.1$). Subsequently, we grouped the trials based on the accuracy of responses (correct and incorrect) and found significant differences between the two groups at approximately 0.6s and 0.7s (Fig. 6b, $t=0.6s$, $p=0.0078$; $t=0.76s$, $p=0.0254$, t-test). When categorizing the data based on both correctness and confidence levels, we found significant differences around 0.4s and 0.7s (Fig.6c, $t=0.44s$, $p=0.0246$; $t=0.76s$, $p=0.0161$, one-way ANOVA). Therefore, by selecting the time point of the maximum T-value and F-value generated by each participant in these categorizations, we discovered that the time required for memory retrieval and metacognition was significantly later compared to that of confidence

generation (Fig.6d, correct vs. incorrect: p=0.0285; High|low×cor|incor: p=0.0151, repeated measures ANOVA, bonferroni's multiple comparison). Based on these results, we can infer that during the process of confidence judgment, the precuneus and the hippocampus play a role in generating confidence at an early time point. Subsequently, the two regions might jointly evaluate the generated confidence, encompassing both the memory retrieval and metacognitive processes. This finding offers valuable insight into our comprehension of confidence generation and metacognition in terms of their temporal progression.

Discussion

We employed intracranial electrode recordings to monitor changes in brain electrical activity in patients with refractory epilepsy during mnemonic metacognitive processes. We delineated the distinct mechanisms underlying the communication between the hippocampus and the precuneus in relation to both confidence and metacognition and elucidated their temporal dynamics. The findings underscore the critical role of a temporal-to-parietal pathway in the genesis of confidence and metacognition, highlighting the importance of neural circuits over isolated brain regions in metacognitive processes.

We provided compelling neuroelectrophysiological evidence of an interaction between the precuneus and hippocampus in mnemonic metacognition. Previous studies have substantiated the involvement of the precuneus in both mnemonic metacognition (McCurdy et al., 2013; Baird et al., 2013; Ye et al., 2018; Ye et al., 2019) and in non-memory domains (Fleming et al. 2010; Heereman et al. 2015; Morales et al., 2018). These past findings point to a role of the precuneus in both memory-related and perceptual metacognition. Pereira et al. (2021) highlights a strong correlation between evidence accumulation and meta-perception in the posterior parietal cortex. However, the constraints of electrocorticography (ECoG) in their study left unresolved whether

deep brain structures such as the hippocampus are implicated during metacognition. Tanglay et al. (2022) showed the fiber bundle connecting the precuneus to the parahippocampal gyrus, providing anatomical evidence for the interaction between the hippocampus and the precuneus. Furthermore, several studies have identified interaction between the hippocampus and the precuneus in various cognition functions, such as memory (Ren et al., 2018), reasoning decisions (Pudhiyidath et al., 2023), and self- and goal-oriented processing (Zheng et al., 2021). In fact, there are suggestions that the hippocampus appears to assume a role in memory-related metacognition (Allen et al., 2017; Miyamoto et al., 2017, 2018; Ye et al., 2019). These findings suggest that the interaction between the hippocampus and the precuneus could pertain to mnemonic metacognition. Our findings are in line with this possibility and characterized the interaction between these cortical-subcortical regions in a metamemory task.

Through the neural communication between the hippocampus and the precuneus, we distinguished between confidence and metacognition, a finding carrying significant theoretical implications. The current consensus suggests that metacognition and confidence generation are distinct cognitive processes (Fleming, 2024; Miyoshi et al., 2024). The task of disentangling the processes of confidence generation from metacognitive evaluation is not trivial. While the majority of studies endeavor to distinguish these processes through the application of computational models (Maniscalco & Lau, 2012; Ratcliff et al., 2016; Adler & Ma, 2018; Miyoshi et al., 2018), our study is the first to empirically differentiate them based on their electrophysiological mechanism and respective time courses. In the following, we will expand on them further.

For distinct neural communication mechanisms, we observed stronger phase amplitude coupling between the precuneus and hippocampus during the confidence rating stage. The phase amplitude coupling phenomenon has been linked to memory processes in humans (Diogo et al., 2022; Saint Amour di Chanaz et al., 2023). A similar phase amplitude coupling was found between the hippocampus and precuneus during memory

retrieval (Hebscher et al., 2019), but here we linked this phenomenon to confidence generation. In our study, the phenomenon of power-related phase-amplitude coupling, characterized by low-frequency band activity in the precuneus and high-frequency band activity in the hippocampus, demonstrated a significant correlation with confidence levels within individual subjects. However, this correlation does not extend to metacognitive abilities in the across-subjects analysis. These characterized bands are congruent with prior research indicating an association of the parietal lobe's theta band with confidence (Yazar et al., 2014; Wynn et al., 2020; Heinbockel et al., 2021), and the involvement of the hippocampus's gamma band in memory-related cognition (Burke et al., 2014; Staresina et al., 2016; Mart, 2021). In an earlier study, theta burst TMS targeted at the posterior inferior parietal cortex can enhance confidence in memory formation (Tambini et al., 2018). This enhancing effect could be attributable to an increase in theta band power within the posterior inferior parietal cortex, consistent with the theta band power increases reported in our study. Through this coupled modulation, the hippocampus and precuneus produce frequency bands that are characteristic of an influence on confidence levels.

Moreover, memory-selective neurons in the hippocampus do show firing patterns linked to confidence judgments (Rutishauser et al., 2015). Similarly, the connection from the hippocampus to the precuneus can predict confidence levels effectively in memory retrieval (Ren et al., 2018). Gray matter myelination in the hippocampus is correlated with individuals' metacognition ability (Allen et al., 2017). Building on these findings on first-order (memory) processes we clarified the neural correlates underpinning metacognitive efficiency and its link to the second-order (confidence) processes. Here, the relationship between the energy in the hippocampus's gamma band and its high correlation with the precuneal gamma band reflect individuals' metacognitive efficiency. We observed that a higher correlation between these regions was positively associated with metacognitive efficiency, while increased gamma band energy was inversely related to it. This dissociation indicates a specific and independent functional role of the hippocampus in comparison to the inter-regional communication.

Moreover, elevated gamma band activity in the hippocampus was also observed during trials with incorrect responses, indicating that the hippocampus may generate an "error signal" during introspective monitoring, in alignment with previous findings (Bastos et al., 2012; Haque et al., 2020; Desender et al., 2021).

Secondly, the fine time course for the computation of confidence generation and metacognitive processes has not been known (Desender et al., 2021; Maniscalco, et al., 2021; Dotan et al., 2018; Fetsch et al., 2018). To elucidate the temporal distinction between confidence and metacognition, we analyzed temporal correlation between the hippocampus and precuneus over the one-second period following the onset of the confidence rating stage. The temporal correlation analysis revealed distinct timing for confidence, memory retrieval, and metacognition. The generation of confidence in meta-perception typically transpires within an extensive temporal frame, spanning from 0.2 to 0.5 seconds (Xue et al., 2023). In alignment with this observation, our results indicate that the genesis of confidence occurs approximately 0.4 seconds following the onset of the confidence phase. This finding underscores the necessity of a substantial time window for the emergence of confidence across both meta-memory and meta-perception domains. Further analyses revealed that the processes of memory retrieval and metacognition are evident approximately 0.7 seconds subsequent to the commencement of the confidence phase, suggesting a sequential progression in cognitive processing stages. We found that the timing with memory retrieval exhibits an almost 0.3 seconds delay compared to the process of confidence generation. By pinpointing and comparing the temporal dynamics of confidence generation and metacognitive processes, we gain insights into how introspective judgment or memory retrieval might be linked to the differences in response time that underpinning choice certainty (Kiani et al., 2014). This cross-regional correlation introduces a novel approach for differentiating between Type 1 and Type 2 tasks temporally (Green & Swets, 1966; Maniscalco & Lau, 2012). This correlation presents new evidence for distinguishing between the generation of confidence and metacognitive processes from a temporal perspective. Further work could also target at examining the time courses

for other related subjective indices such as the generation of vividness in memory (Zou & Kwok, 2022).

In conclusion, our research has differentiated between confidence and metacognition by examining brain electrical activities and their distinct characteristics underlying these two cognitive processes. In light of its relationship with the precuneus, we found that the hippocampus should be considered as a crucial structure in metacognition. Our findings provide robust empirical data for existing computational models and introduce a novel perspective on how the parietal-hippocampal circuit is warranted for metacognitive research.

REFERENCE

1. Adler, W. T., & Ma, W. J. (2018). Comparing Bayesian and non-Bayesian accounts of human confidence reports. *PLoS Computational Biology*, *14*(11). https://doi.org/10.1371/journal.pcbi.1006572
2. Allen, M., Glen, J. C., Müllensiefen, D., Schwarzkopf, D. S., Fardo, F., Frank, D., Callaghan, M. F., & Rees, G. (2017). Metacognitive ability correlates with hippocampal and prefrontal microstructure. *NeuroImage*, *149*, 415–423. https://doi.org/10.1016/j.neuroimage.2017.02.008
3. Baird, B., Smallwood, J., Gorgolewski, K. J., & Margulies, D. S. (2013). Medial and lateral networks in anterior prefrontal cortex support metacognitive ability for memory and perception. *Journal of Neuroscience*, *33*(42), 16657–16665. https://doi.org/10.1523/JNEUROSCI.0786-13.2013
4. Bicanski, A., & Burgess, N. (2018). A neural-level model of spatial memory and imagery. *ELife*, *7*. https://doi.org/10.7554/eLife.33752
5. Burke, J. F., Long, N. M., Zaghloul, K. A., Sharan, A. D., Sperling, M. R., & Kahana, M. J. (2014). NeuroImage Human intracranial high-frequency activity maps episodic memory formation in space and time. *NeuroImage*, *85*, 834–843. https://doi.org/10.1016/j.neuroimage.2013.06.067
6. Cai, Y., Jin, Z., Zhai, C., Wang, H., Wang, J., Tang, Y., & Kwok, S. C. (2022). Time-sensitive prefrontal involvement in associating confidence with task performance illustrates metacognitive introspection in monkeys. *Communications Biology*, *5*(1). https://doi.org/10.1038/s42003-022-03762-6
7. Canolty, R. T., Edwards, E., Dalal, S. S., Soltani, M., Nagarajan, S. S., Kirsch, H. E., Berger, M. S., Barbare, N. M., & Knight, R. T. (2006). High gamma power is phase-locked to theta oscillations in human neocortex. *Science*, *313*(5793), 1626–1628. https://doi.org/10.1126/science.1128115
8. Das, A., & Menon, V. (2023). *Hippocampal-parietal cortex causal information flow in human episodic memory : replication across three experiments*.
9. Desender, K., Donner, T. H., & Verguts, T. (2021). Dynamic expressions of confidence within an evidence accumulation framework. *Cognition*, *207*.

https://doi.org/10.1016/j.cognition.2020.104522

10. Desender, K., Ridderinkhof, K. R., & Murphy, P. R. (2021). Understanding neural signals of post-decisional performance monitoring: An integrative review. *ELife*, *10*, 1–21. https://doi.org/10.7554/eLife.67556
11. Dotan, D., Meyniel, F., & Dehaene, S. (2018). On-line confidence monitoring during decision making. *Cognition*, *171*, 112–121. https://doi.org/10.1016/j.cognition.2017.11.001
12. Fetsch, C. R., Odean, N. N., Jeurissen, D., El-Shamayleh, Y., Horwitz, G. D., & Shadlen, M. N. (n.d.). *Focal optogenetic suppression in macaque area MT biases direction discrimination and decision confidence, but only transiently*. https://doi.org/10.7554/eLife.36523.001
13. Flavell, J. H. (1979). Metacognition and cognitive monitoring: A new area of cognitive–developmental inquiry. American Psychologist, 34(10), 906–911.
14. Fleming, Stephen M; Weil, Rimona S; Nagy, Zoltan; Dolan, Raymond J; & Rees, G. (2010). Tackling Attack Detection and Incident Response. *Science*, *329*(April), 1541–1543. https://doi.org/10.1126/science.1191883.Relating
15. Fleming, S. M. (2024). Metacognition and Confidence: A Review and Synthesis. *Annual Review of Psychology*, *75*(1), 1–28. https://doi.org/10.1146/annurev-psych-022423-032425
16. Fleming, S. M., & Daw, N. D. (2017). Self-evaluation of decision-making: A general bayesian framework for metacognitive computation. *Psychological Review*, *124*(1), 91–114. https://doi.org/10.1037/rev0000045
17. Fleming, S. M., & Lau, H. C. (2014). How to measure metacognition. In *Frontiers in Human Neuroscience* (Vol. 8, Issue JULY). Frontiers Media S. A. https://doi.org/10.3389/fnhum.2014.00443
18. Foudil, S. A., Kwok, S. C., & Macaluso, E. (2020). Context-dependent coding of temporal distance between cinematic events in the human precuneus. *Journal of Neuroscience*, *40*(10). https://doi.org/10.1523/JNEUROSCI.2296-19.2020
19. Futing Zou, Sze Chai Kwok; Distinct Generation of Subjective Vividness and Confidence during Naturalistic Memory Retrieval in Angular Gyrus. J Cogn Neurosci 2022; 34 (6): 988–1000. doi: https://doi.org/10.1162/jocn_a_01838
20. Green, D.M., Swets, J.A., 1966. Signal Detection Theory and Psychophysics. John Wiley, Oxford.
21. Haque, R. U., Inati, S. K., Levey, A. I., & Zaghloul, K. A. (n.d.). *episodic memory retrieval*. *2020*, 1–14. https://doi.org/10.1038/s41467-020-19828-0
22. Hebart, M. N., Schriever, Y., Donner, T. H., & Haynes, J. D. (2016). The Relationship between Perceptual Decision Variables and Confidence in the Human Brain. *Cerebral Cortex*, *26*(1), 118–130. https://doi.org/10.1093/cercor/bhu181
23. Hebscher, M., Ibrahim, C., & Gilboa, A. (2020). Precuneus stimulation alters the neural dynamics of autobiographical memory retrieval. *NeuroImage*, *210*(June 2019), 116575. https://doi.org/10.1016/j.neuroimage.2020.116575
24. Hebscher, M., Meltzer, J. A., & Gilboa, A. (2019). A causal role for the precuneus in network-wide theta and gamma oscillatory activity during complex memory retrieval. *ELife*, *8*, 1–20. https://doi.org/10.7554/eLife.43114
25. Heereman, J., Walter, H., & Heekeren, H. R. (2015). A task-independent neural representation of subjective certainty in visual perception. *Frontiers in Human Neuroscience*, *9*(OCT). https://doi.org/10.3389/fnhum.2015.00551
26. Heinbockel, H., Quaedflieg, C. W. E. M., Schneider, T. R., Engel, A. K., & Schwabe, L. (2021).

Stress enhances emotional memory-related theta oscillations in the medial temporal lobe. *Neurobiology of Stress*, *15*, 100383. https://doi.org/10.1016/j.ynstr.2021.100383

27. Hemptinne, C. De, Swann, N. C., Ostrem, J. L., Ryapolova-webb, E. S., Luciano, M. S., Galifianakis, N. B., & Starr, P. A. (2015). *Therapeutic deep brain stimulation reduces cortical phase-amplitude coupling in Parkinson ' s disease*. *18*(5). https://doi.org/10.1038/nn.3997
28. Kiani, R., Corthell, L., & Shadlen, M. N. (2014). Choice certainty is informed by both evidence and decision time. *Neuron*, *84*(6), 1329–1342. https://doi.org/10.1016/j.neuron.2014.12.015
29. Maniscalco, B., & Lau, H. (2012). A signal detection theoretic approach for estimating metacognitive sensitivity from confidence ratings. *Consciousness and Cognition*, *21*(1), 422–430. https://doi.org/10.1016/j.concog.2011.09.021
30. Maniscalco, B., Odegaard, B., Grimaldi, P., Cho, S. H., Basso, M. A., Lau, H., & Peters, M. A. K. (2021). Tuned inhibition in perceptual decision-making circuits can explain seemingly suboptimal confidence behavior. *PLoS Computational Biology*, *17*(3), 1–28. https://doi.org/10.1371/journal.pcbi.1008779
31. Mart, C. (2021). *The hippocampus as the switchboard between perception and memory*. *118*(50). https://doi.org/10.1073/pnas.2114171118/-/DCSupplemental.Published
32. McCurdy, L. Y., Maniscalco, B., Metcalfe, J., Liu, K. Y., de Lange, F. P., & Lau, H. (2013). Anatomical coupling between distinct metacognitive systems for memory and visual perception. *Journal of Neuroscience*, *33*(5), 1897–1906. https://doi.org/10.1523/JNEUROSCI.1890-12.2013
33. Miyamoto K, Osada T, Setsuie R, Takeda M, Tamura K, Adachi Y, Miyashita Y. Causal neural network of metamemory for retrospection in primates. Science. 2017 Jan 13;355(6321):188-193. doi: 10.1126/science.aal0162. PMID: 28082592.
34. Miyamoto, K., Setsuie, R., Osada, T., & Miyashita, Y. (2018). Reversible Silencing of the Frontopolar Cortex Selectively Impairs Metacognitive Judgment on Non-experience in Primates. Neuron, 97(4), 980-989.e6. https://doi.org/10.1016/j.neuron.2017.12.040
35. Miyoshi, K., Kuwahara, A., Kawaguchi, J., 2018. Comparing the confidence calculation rules for forced-choice recognition memory: A winner-takes-all rule wins. J. Mem. Lang. 102, 142–154. https://doi.org/10.1016/j.jml.2018.06.001
36. Miyoshi, K., Webb, T., Rahnev, D., & Lau, H. (2024). Confidence and metacognition. In *Reference Module in Neuroscience and Biobehavioral Psychology*. Elsevier. https://doi.org/10.1016/b978-0-12-820480-1.00049-8
37. Morales, J., Lau, H., & Fleming, S. M. (2018). Domain-general and domain-specific patterns of activity supporting metacognition in human prefrontal cortex. *Journal of Neuroscience*, *38*(14), 3534–3546. https://doi.org/10.1523/JNEUROSCI.2360-17.2018
38. Pereira, M., Megevand, P., Tan, M. X., Chang, W., Wang, S., Rezai, A., Seeck, M., Corniola, M., Momjian, S., Bernasconi, F., Blanke, O., & Faivre, N. (2021). Evidence accumulation relates to perceptual consciousness and monitoring. *Nature Communications*, *12*(1), 1–11. https://doi.org/10.1038/s41467-021-23540-y
39. Pouget, A., Drugowitsch, J., & Kepecs, A. (2016). Confidence and certainty: Distinct probabilistic quantities for different goals. In *Nature Neuroscience* (Vol. 19, Issue 3, pp. 366–374). Nature Publishing Group. https://doi.org/10.1038/nn.4240
40. Pudhiyidath, A., Morton, N. W., Duran, R. V., Schapiro, A. C., Momennejad, I., Hinojosa-Rowland, D. M., Molitor, R. J., & Preston, A. R. (2022). Representations of Temporal Community Structure in Hippocampus and Precuneus Predict Inductive Reasoning Decisions. *Journal of Cognitive*

Neuroscience, *34*(10), 1736–1760. https://doi.org/10.1162/jocn_a_01864

41. Ratcliff, R., Smith, P. L., Brown, S. D., & McKoon, G. (2016). Diffusion Decision Model: Current Issues and History. In *Trends in Cognitive Sciences* (Vol. 20, Issue 4, pp. 260–281). Elsevier Ltd. https://doi.org/10.1016/j.tics.2016.01.007
42. Ren, Y., Nguyen, V. T., Sonkusare, S., Lv, J., Pang, T., Guo, L., Eickhoff, S. B., Breakspear, M., & Guo, C. C. (2018). Effective connectivity of the anterior hippocampus predicts recollection confidence during natural memory retrieval. *Nature Communications*, *9*(1). https://doi.org/10.1038/s41467-018-07325-4
43. Rutishauser, U., Ye, S., Koroma, M., Tudusciuc, O., Ross, I. B., Chung, J. M., & Mamelak, A. N. (2015). Representation of retrieval confidence by single neurons in the human medial temporal lobe. *Nature Neuroscience*, *18*(7), 1041–1050. https://doi.org/10.1038/nn.4041
44. Shekhar, M., & Rahnev, D. (2018). Distinguishing the roles of dorsolateral and anterior PFC in visual metacognition. *Journal of Neuroscience*, *38*(22), 5078–5087. https://doi.org/10.1523/JNEUROSCI.3484-17.2018
45. Staresina, B. P., Michelmann, S., Bonnefond, M., Jensen, O., Axmacher, N., & Fell, J. (2016). *Hippocampal pattern completion is linked to gamma power increases and alpha power decreases during recollection*. 1–18. https://doi.org/10.7554/eLife.17397
46. Saint Amour di Chanaz L, Pérez-Bellido A, Wu X, Lozano-Soldevilla D, Pacheco-Estefan D, Lehongre K, Conde-Blanco E, Roldan P, Adam C, Lambrecq V, Frazzini V, Donaire A, Carreño M, Navarro V, Valero-Cabré A, Fuentemilla L. Gamma amplitude is coupled to opposed hippocampal theta-phase states during the encoding and retrieval of episodic memories in humans. Curr Biol. 2023 May 8;33(9):1836-1843.e6. doi: 10.1016/j.cub.2023.03.073. Epub 2023 Apr 14. PMID: 37060906.
47. Santos-Pata D., Zucca R., Fernandez Amil A., Principe A., Pérez-Enríquez C., Rocamora R., Kwok S. C., Verschure P. (2022). Theta oscillations in the human hippocampus normalize the information content of episodic memory. bioRxiv preprint. https://doi.org/10.1101/2022.06.27.497705
48. Tanglay, O., Young, I. M., Dadario, N. B., Briggs, R. G., Fonseka, R. D., Dhanaraj, V., Hormovas, J., Lin, Y. H., & Sughrue, M. E. (2022). Anatomy and white-matter connections of the precuneus. In *Brain Imaging and Behavior* (Vol. 16, Issue 2, pp. 574–586). https://doi.org/10.1007/s11682-021-00529-1
49. Tort, A. B. L., Kramer, M. A., Thorn, C., Gibson, D. J., Kubota, Y., Graybiel, A. M., & Kopell, N. J. (2008). *Dynamic cross-frequency couplings of local field potential oscillations in rat striatum and hippocampus during performance of a T-maze task. 105*(51), 20517–20522. https://doi.org/10.1073/pnas.0810524105
50. Wynn, S. C., Kessels, R. P. C., & Schutter, D. J. L. G. (2020). Effects of parietal exogenous oscillatory field potentials on subjectively perceived memory confidence. *Neurobiology of Learning and Memory*, *168*(June 2019). https://doi.org/10.1016/j.nlm.2019.107140
51. Xue, K., Zheng, Y., Rafiei, F., & Rahnev, D. (2023). The timing of confidence computations in human prefrontal cortex. *Cortex*, 1–28. https://doi.org/10.1016/j.cortex.2023.08.009
52. Yazar, Y., Bergström, Z. M., & Simons, J. S. (2014). Continuous theta burst stimulation of angular gyrus reduces subjective recollection. *PLoS ONE*, *9*(10). https://doi.org/10.1371/journal.pone.0110414
53. Ye, Q., Zou, F., Dayan, M., Lau, H., Hu, Y., & Kwok, S. C. (2019). Individual susceptibility to TMS affirms the precuneal role in meta-memory upon recollection. *Brain Structure and Function*,

224(7), 2407–2419. https://doi.org/10.1007/s00429-019-01909-6

54. Ye, Q., Zou, F., Lau, H., Hu, Y., & Kwok, S. C. (2018). Causal evidence for mnemonic metacognition in human precuneus. *Journal of Neuroscience*, *38*(28), 6379–6387. https://doi.org/10.1523/JNEUROSCI.0660-18.2018

55. Yin, Z., Zhu, G., Liu, Y., Zhao, B., Liu, D., Bai, Y., Zhang, Q., Shi, L., Feng, T., Yang, A., Liu, H., Meng, F., Neumann, W. J., Kühn, A. A., Jiang, Y., & Zhang, J. (2022). Cortical phase-Amplitude coupling is key to the occurrence and treatment of freezing of gait. *Brain*, *145*(7), 2407–2421. https://doi.org/10.1093/brain/awac121

56. Zheng, A., Montez, D. F., Marek, S., Gilmore, A. W., Newbold, D. J., Laumann, T. O., Kay, B. P., Seider, N. A., Van, A. N., Hampton, J. M., Alexopoulos, D., Schlaggar, B. L., Sylvester, C. M., Greene, D. J., Shimony, J. S., Nelson, S. M., Wig, G. S., Gratton, C., McDermott, K. B., … Dosenbach, N. U. F. (2021). Parallel hippocampal-parietal circuits for self- And goal-oriented processing. *Proceedings of the National Academy of Sciences of the United States of America*, *118*(34). https://doi.org/10.1073/pnas.2101743118

57. Zuo, S., Wang, L., Shin, J. H., Cai, Y., Lee, S. W., Appiah, K., Zhou, Y. Di, & Kwok, S. C. (2020). Behavioral evidence for memory replay of video episodes in the macaque. *ELife*, *9*, 1–23. https://doi.org/10.7554/eLife.54519

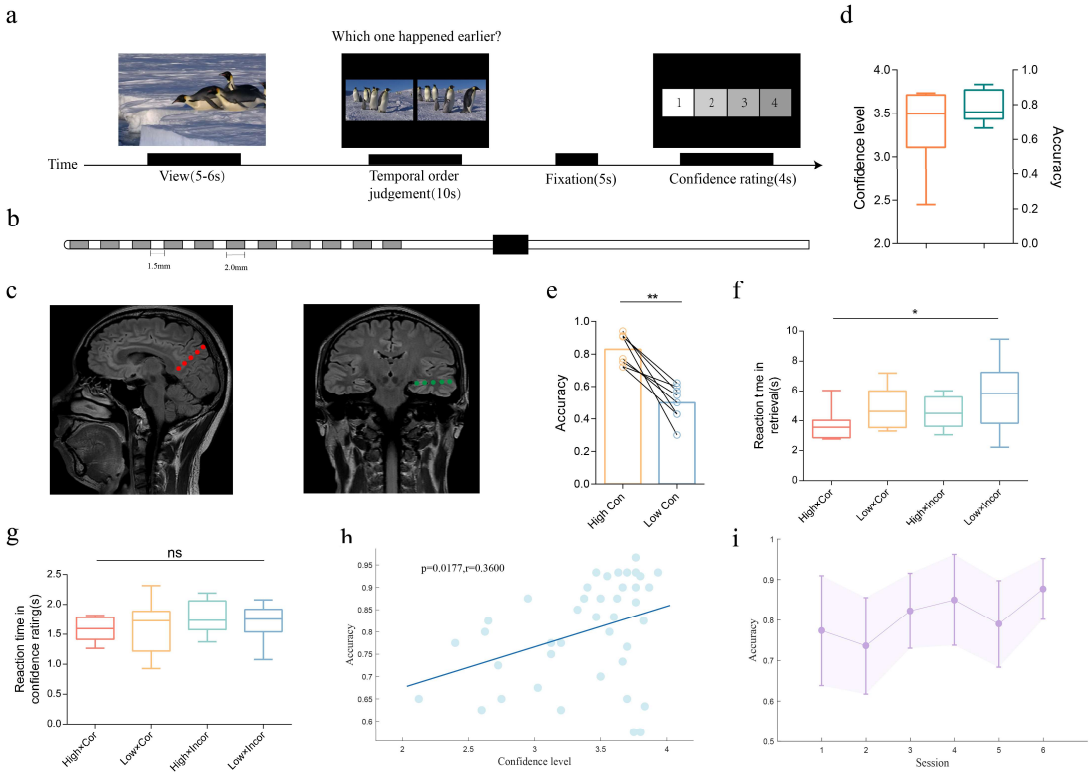

Figure 1. Experimental design, electrodes location and behavioral details. (a) Experimental design. Participants performed a temporal order judgment task, by choosing the image that happened earlier in the video. After this, participants needed to report confidence level from 1-4 points. (b) Schematic diagram of stereoelectroencephalography electrodes used in this study. (c) An example trajectory of two intracranial electrodes in the precuneus and the hippocampus, respectively. (d) Bar plot shows average confidence level (3.58±0.19) and average accuracy (0.79±0.094) and mean confidence level across participants. (e) Box plot shows the average reaction time in the retrieval stage (Friedman test, p=0.0181). The reaction time in high×correct is significantly shorter than low×incorrect by multiple comparisons (p=0.0117). (f) Bar plot shows the accuracy in high confidence and low confidence (Wilcoxon test, p=0.0078). (g) Box plot shows the average reaction time in the confidence rating stage. (h) The correlation between the confidence level and accuracy across patients. Each dot denotes a session. (i) The Average± SEM (across participants) of the accuracy across experimental sessions.

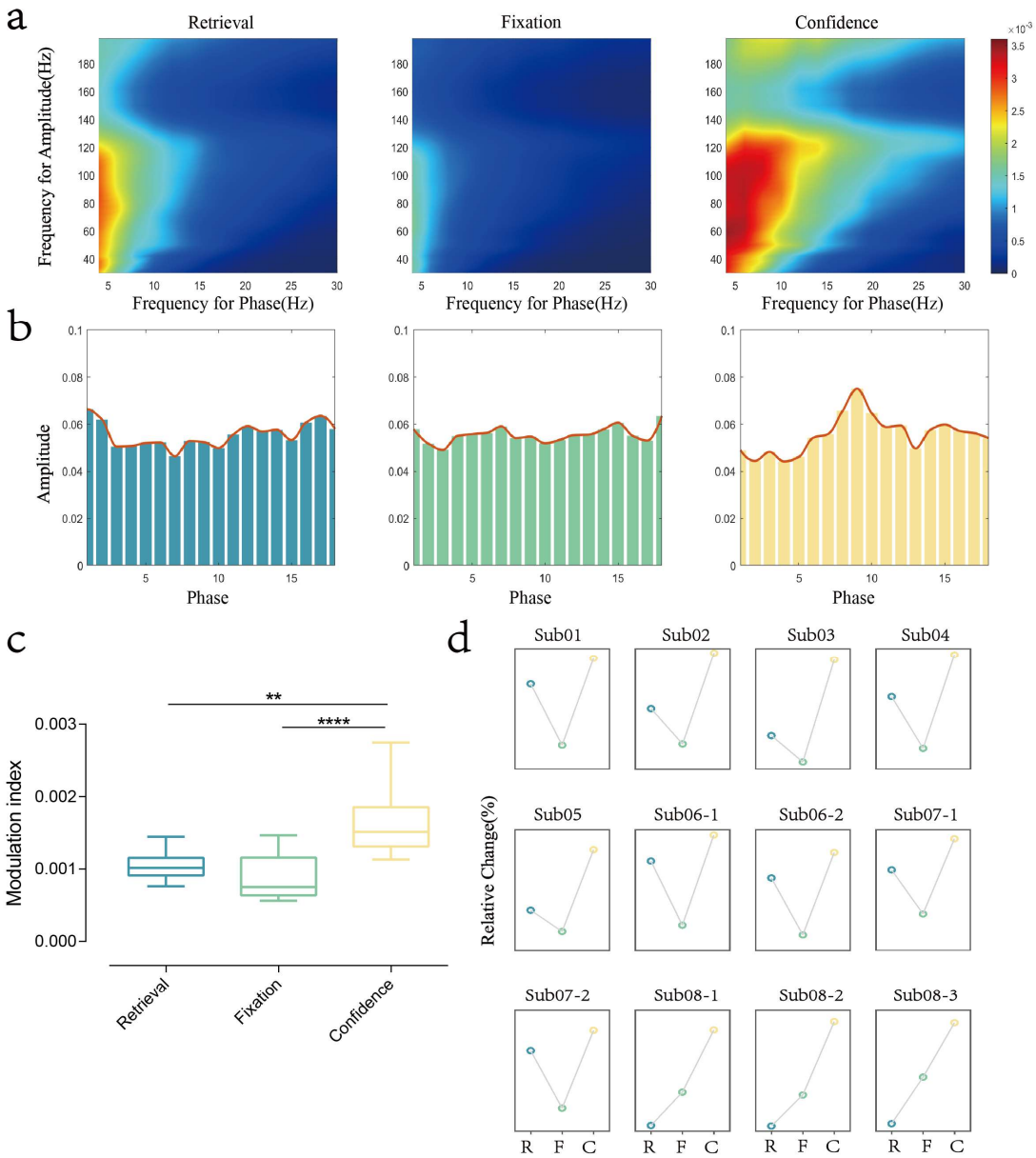

Figure 2. Confidence rating stage has a stronger phase amplitude coupling (PAC) than other stages. (a) Representative example of PAC observed in precuneus (phase) and hippocampus (amplitude) of one subject in retrieval (left), fixation (middle), confidence (right). The warmest colors represent the strongest coupling. The amplitude frequency ranges from 30-200Hz, and phase frequency ranges from 4-30Hz. (b) Examples show the distributions of amplitude and preferred phase of the coupling in retrieval (left), fixation (middle), confidence (right). (c) Box plot shows the PAC in three periods (Friedman test, retrieval: $p=0.0066$, fixation: $p<0.0001$). (d) A similar pattern of PAC change is shown in all subjects, showing higher coupling in the confidence rating stage. R: retrieval; F: fixation; C: confidence rating.

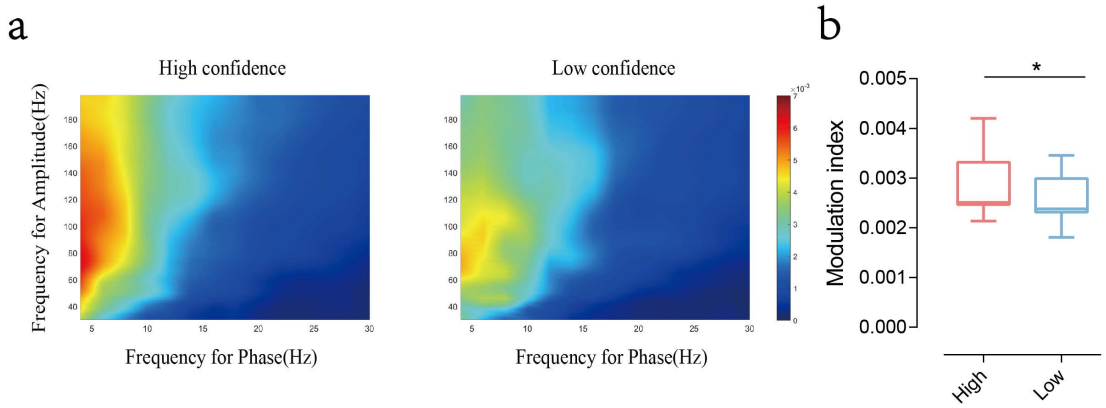

Figure 3. High confidence trials have stronger phase-amplitude coupling compared with low confidence trials. (a) Representative example of PAC observed in high confidence level (left) versus low confidence level (right). The amplitude frequency ranges from 30-200Hz, and phase frequency ranges from 4-30Hz. (b) Box plot shows the mean PAC (30-100Hz for amplitude and 4-10 Hz for phase) in high confidence compared with low confidence (signed-rank test, p=0.0269).

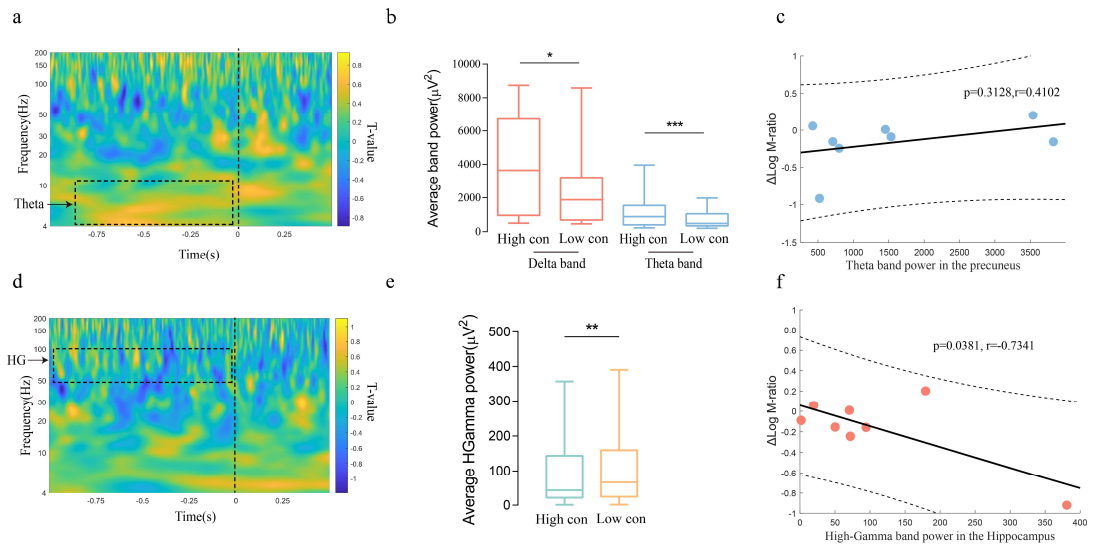

Figure 4. Stronger phase amplitude coupling is related with higher power in the precuneus and hippocampus (a) Time-frequency analysis (T-value map) contrasting high confidence trials with low confidence trials, averaged across all participants in the precuneus. The dashed line indicates the time point of reporting confidence level. Positive T-value refers to increased power in high confidence trials. The threshold of the T-value map is at $P < 0.05$. (b) Box plot shows the average Delta and Theta power in the precuneus during the confidence rating stage (paired signed-rank test, delta: p=0.0161, theta: p=0.0005). (c) The metacognitive efficiencies (log(meta-d'/d')) exhibited no significant correlation with theta band power in the precuneus during the confidence rating stage (r=0.4102, p=0.3128). (d) Time-frequency analysis (T-value map) of high confidence trials compared with low confidence trials from the time point of reporting confidence level (dashed vertical line) averaged across all participants in the hippocampus. Negative T-value refers to decreased power in high confidence trials. The threshold of the T-value map is at $P < 0.05$. HG: High-Gamma. (e) Box plot shows the average high-gamma power in the hippocampus during the reporting confidence stage (high confidence versus low confidence, paired signed-rank test, p=0.0078). (f) The metacognitive efficiencies (log(meta-d'/d')) were significantly correlated with high-gamma band power negatively in the hippocampus during the confidence rating stage (r=-0.7341, p=0.0381).

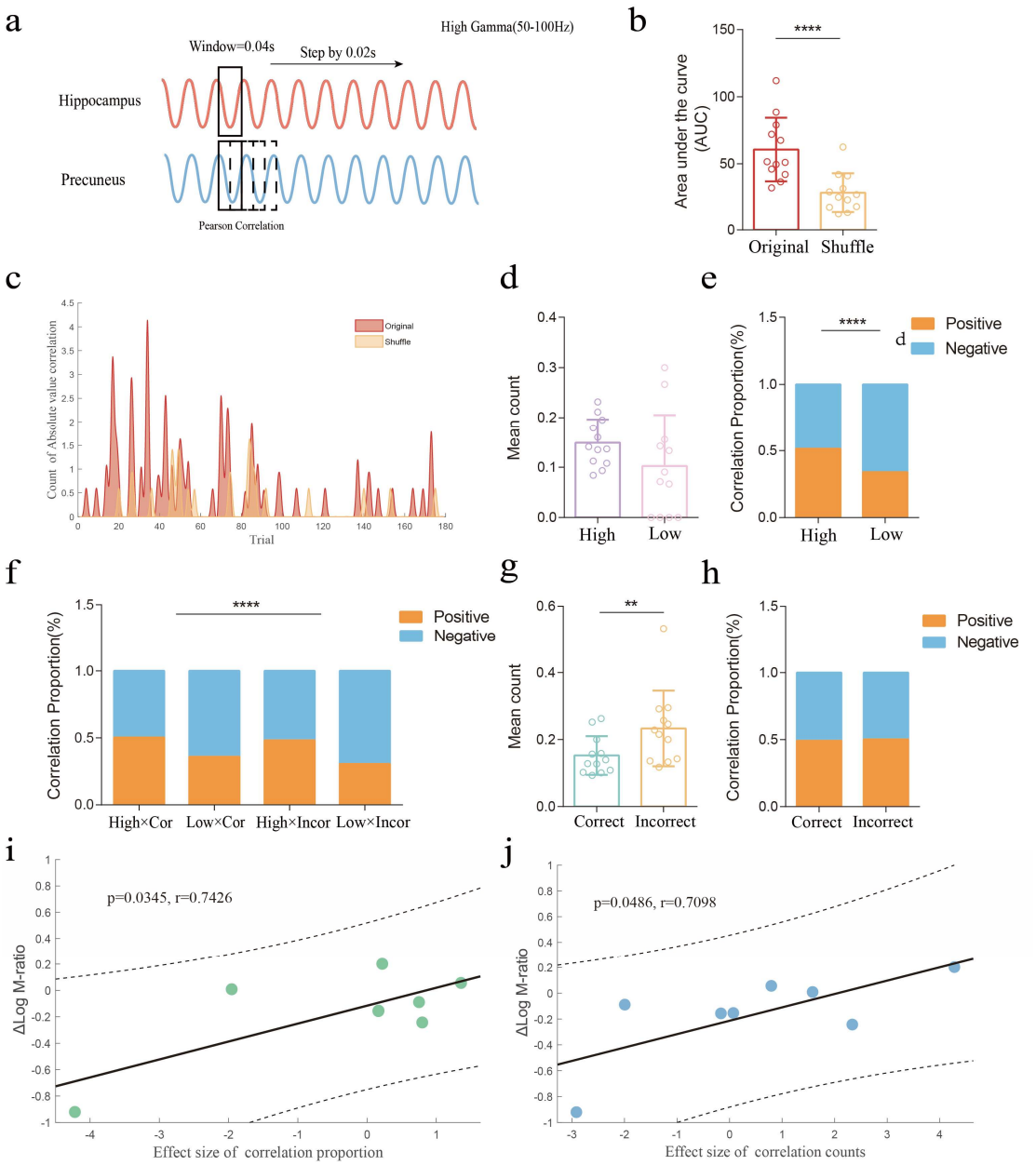

Figure 5. Correlation analysis between the precuneus and the hippocampus in the confidence rating stage. (a) Schematic diagram of correlation analysis procedure. We defined a 0.04s length window, step by 0.02s, and calculated Person correlation in each window. Segments in which 4 or more consecutive windows showing significant correlation are considered high correlation. (b) Bar plot shows area under the curve (AUC) of original and shuffled data (paired t-test, $p<0.0001$). (c) Representative example of significant correlation frequency (absolute value) per trial. Distribution in red refers to the real data, distribution in yellow refers to the shuffled data. (d) Bar plot shows mean count in two different conditions (high confidence versus low confidence, paired t-test, $p=0.1477$). (e) Bar plot shows the correlation proportion in high confidence versus low confidence (Chi-square test, $p<0.0001$). (f) Bar plot shows the correlation proportion in four different conditions (high confidence × correct, low confidence × correct, high confidence × incorrect, low confidence × incorrect, Chi-square test, $p<0.0001$). (g) Bar plot shows mean count in two different conditions (correct versus incorrect, signed-rank test, $p=0.0049$). (h) Bar plot shows the correlation proportion in correct versus incorrect. (i) The effect size of correlation proportion is significantly correlated positively with M-ratio ($r=0.7426$, $p=0.0345$). (j) The effect size of correlation count is significantly correlated positively with M-ratio ($r=0.7098$, $p=0.0486$).

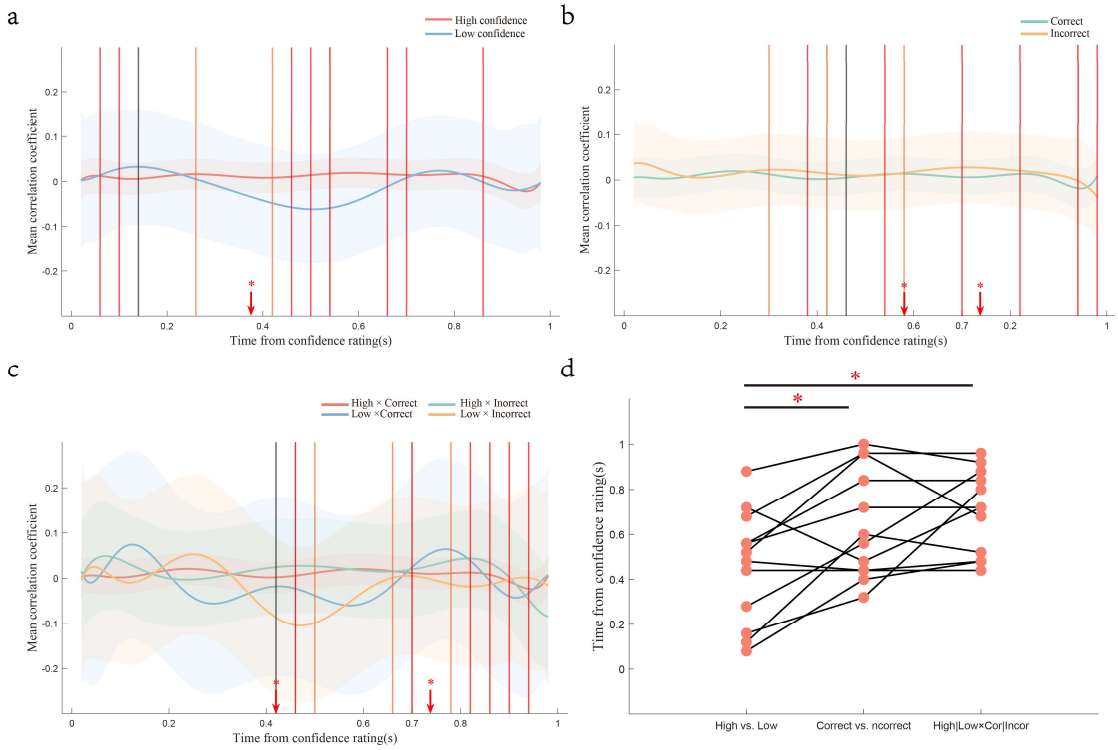

Figure 6. The time course of correlation in confidence generation precedes retrieval and metacognition. (a) The average correlation coefficient within 1 second after the onset of confidence rating across participants in high confidence trials compared with low confidence trials. The asterisk represent the significance of the average level (p=0.0399, t-test). The vertical line represents the time point with the maximum t-value for each participant (red: p<0.05, orange: p<0.1, black: p>0.1, t-test). (b) The average correlation coefficient within 1 second after the onset of confidence rating across participants in correct trials compared with incorrect trials. The asterisks represent the significance of the average level (first one: t=0.6s, p=0.0078, t-value=2.927; second one: t=0.76s, p=0.0254, t-value=2.398, t-test). The vertical line represents the time point with the maximum t-value for each participant (red: p<0.05, orange: p<0.1, black: p>0.1, t-test). (c) The average correlation coefficient within 1 second after the onset of confidence rating across participants in the four conditions. The asterisks represent the significance of the average level (first one: t=0.44s, p=0.0246; second one: t=0.76s, p=0.0161, one-way ANOVA). The vertical line represents the later time point with the maximum t-value for each participant at the same p-value level (red: p<0.05, orange: p<0.1, black: p>0.1, one-way ANOVA). (d) The scatter plot shows the time points with the maximum t-value under different conditions (correct vs. incorrect: p=0.0285; High|low×cor|incor: p=0.0151, repeated-measures ANOVA, corrected for bonferroni's multiple comparison).

740 ## *METHODS AND MATERIALS*

741

742 ***Participants***

743 Eight patients diagnosed with intractable epilepsy underwent implantation of subdural
744 intracranial electrodes for epilepsy treatment at The Second Affiliated Hospital,
745 Zhejiang University School of Medicine (SAHZU). The patients' ages ranged from 12
746 to 39 (mean=24.5, SD=9.1). All patients demonstrated a good understanding of the
747 experimental procedure and had at least 1 electrode recording signals in both
748 hippocampus and precuneus brain regions. No clinical seizures were observed during
749 the course of the experiment. This study was approved by the SAHZU committee on
750 Human Research.

751

752 ***Experimental task***

753 Each trial began with a video of animals, categorized as either primates or non-primates,
754 which lasted for 5-6 s. These videos were validated in previous studies (Zuo et al., 2020).
755 Subsequently, at the memory test, the participants had to determine which image
756 extracted from the video was presented earlier within a 10-second timeframe (temporal
757 order judgment, TOJ). Following the memory test, a fixation cross was presented for 5
758 s. In the final phase, participants reported their confidence level on a scale ranging from
759 1 to 4. The number of trials completed by each participant varied, with a range of 120-
760 240 trials (4-6 sessions, 30-40 trials per session). Initiation of each trial was self-paced
761 and the participants were allowed to take breaks between sessions as desired.

762

763 ***Intracranial recordings and electrode localization***

764 Recording sites in the subdural grids and strips were 2mm platinum disks with 1.5mm
765 intercontact spacing. Recording sites in depth electrodes implanted in the hippocampus
766 and precuneus were 2-mm platinum cylinders with 3.5-mm intercontact spacing and a
767 diameter of 0.8 mm (Fig.1b). Before electrode implantation, T1-weighted Magnetic
768 Resonance Imaging (MRI) using a 1.5-T scanner and computed tomography were

obtained for each patient. The locations of the electrodes were determined based on clinical standards, utilizing the SINOVATION software. We focused and analyzed only electrodes localized to the hippocampus and precuneus in this study. The specific number of electrodes for each patient is shown in the supplementary table S1.

Preprocessing and data analysis

All data analyses were performed in MATLAB 2020a using EEGLAB, procedure from GitHub and Self-defining script. The sample rate of signal was at 2000 Hz. First, we extracted markers of each event, excluding trials with missing or wrong markers from further analysis. Then bipolar reference was applied to raw data of hippocampus and precuneus by pairing the nearest electrode. We used FIR band-stop filters to remove 50-HZ power line interference. In this study, we focused on three events in the experimental task: 1. TOJ test (10s, retrieval); 2. Rest/Fixation (5s); 3. Report confidence level (4s, confidence rating).

Phase Amplitude Coupling (PAC). Phase-amplitude coupling was calculated using a method described in previous studies (Canolty et al., 2006; Tort et al., 2008; Hemptinne et al., 2015; Yin et al., 2022). Firstly, sEEG signals were bandpass filtered using a FIR filter implemented with the filtfilt function in MATLAB. The low-frequency band was filtered from 4 to 30 Hz, with a 2 Hz step (without overlap), while the high-frequency band was filtered from 30 to 200 Hz, with a 4 Hz step (without overlap). Next, the Hilbert transform was applied to obtain the instantaneous phase and instantaneous amplitude from the low- and high-frequency filtered signals, respectively. The phase was divided into 18 bins, each spanning 20°, and the amplitude envelope was calculated for each bin to generate a distribution of phase-amplitude coupling. The Modulation Index (MI) was then computed using the Kullback-Leibler (KL) distance to quantify the strength of phase-amplitude coupling. Coupling was computed for multiple frequency combinations, with the phase frequencies plotted on the x-axis and the amplitude frequencies on the y-axis.

Correlation Analysis. We used Pearson correlation to examine the relationship between the hippocampus and precuneus during the reporting of confidence levels. Firstly, we extracted the high-gamma (50-100Hz) band from both the hippocampus and precuneus. We then defined a window length of 0.04s, step by 0.02s, and calculated the Pearson correlation coefficient for each window. To ensure the sensitivity and specificity of the results, we considered the signals to be relevant only when all four windows (equivalent to 0.08s) met the minimum criteria of pearson correlation ($r>0.9$, $p<0.05$). The occurrence of highly relevant signals during confidence rating was counted. We quantified the count of high correlation bands within the confidence rating time period, disregarding the specific time series. As a control, we shuffled the trials to establish a baseline for each participant for statistical inference. The shuffling criteria were as follows: 1) random matching of signals from different trials, 2) a minimum interval of 10 trials between shuffled signals, and 3) ensuring that the category of video for shuffled trials differs. Subsequently, we calculated the average frequency for each subject in both the original and shuffled data. Finally, we applied a paired Wilcoxon test for frequency and chi-square test for correlation proportion to detect significance ($p<0.05$). Regarding the correlation within time series, a window width of 0.04 s was also utilized to compute the correlation of gamma frequency bands at each time point. T-tests were conducted to explore the disparities in the average correlation coefficients between the two groups for each time point, as well as the differences for each subject. Analysis of variance (ANOVA) was employed to evaluate the distinction among the four groups. Subsequently, in single factor classification analysis, the time point for each subject is determined by identifying the point with the highest t-statistic. Conversely, in two factors classification analysis, the selection criteria for the time point is adjusted to identify a marginally later time point, while maintaining the same level of statistical significance.

Measurement of metacognitive efficiency. Building upon prior research, we computed type 1 sensitivity (d') and type 2 sensitivity (meta-d'), wherein meta-d' indicates metacognitive sensitivity and d' represents memory performance according to signal

detection theory (Green and Swets, 1966; Maniscalco and Lau,2012). We compared meta-d' with d' (M-ratio: meta-d'/d') for each participant to estimate metacognitive efficiency employing a hierarchical Bayesian estimation method (Fleming and Lau, 2014; Fleming and Daw, 2017). Adhering to a standard approach, we divided within-subjects trials by their confidence levels into two categories for analysis: High confidence (3-4), Low confidence (1-2).

Power Spectral Density (PSD). In three stages (retrieval, fixation, confidence rating), we calculated PSD with Welch periodogram method (pwelch function in MATLAB) for the time from the start to pressing the button, using the Hanning window and 50% overlap to reduce edge effects. The following frequency band are calculated (bandpower function in MATLAB): delta (1–4Hz), theta (4–8Hz), alpha (8–14 Hz), beta (14–20 Hz), low-gamma (30-50 Hz), and high-gamma (50-100 Hz). Then we compare different frequency band power in different groups according to high and low confidence level or correct and incorrect responses.

Time–frequency analysis. Time–frequency analyses were carried out using the Morlet wavelet transform method (cwt function in MATLAB) with default scale. We then computed the corresponding T values for each participant, which we averaged across participants in different conditions.

ACKNOWLEDGEMENT

We are grateful to the patients for their kind cooperation. K.P, thanks Hongyi Ye and Xiaobo Yu for their helpful suggestions in data analysis and statistical analysis. We thank medical staff involved in clinical treatment and technicians in the EEG laboratories.

AUTHOR CONTRIBUTIONS

Hongjie Jiang and Sze Chai Kwok conceived the study and designed the experiment. Kai Pan and Xinxia Guo analyzed the data. Jianmin Zhang supervised the surgeries and experiments. Kai Pan and Zhoule Zhu ran the experiments. Zhe Zheng, Junming Zhu, and Hongjie Jiang performed the surgeries and contributed to electrode localization. Kai Pan and Hongjie Jiang wrote the paper. Hemmings Wu, Diogo Santos-Pata, and Sze Chai Kwok further interpreted the data and contributed to the writing by reviewing and editing the manuscript.

COMPETING INTERESTS

The authors declare no competing financial interests.

FUNDING

S.C.K. received support from the National Natural Science Foundation of China (grant number: 32071060), Jiangsu Provincial Department of Science and Technology (grant number: BK20221267), and Open Research Fund of the State Key Laboratory of Cognitive Neuroscience and Learning (Beijing Normal University).